Design of heat sinks for wearable thermoelectric generators to power personal heating garments: A numerical study

Design of heat sinks for wearable thermoelectric generators to power personal heating garments: A numerical study

Z Soleimani[1*], S Zoras[1], Y Cui[1], B Ceranic[1] and S Shahzad[2]

[1]Department of Built Environment, College of Engineering and Technology, University of Derby, DE22 3AW, Derby, UK

[2] Sheffield School of Architecture, University of Sheffield, S10 2TN, Sheffield, UK

[*]Email: z.soleimani@derby.ac.uk

Abstract. To mitigate climate change attributed to the built environments, there have been tremendous efforts to improve air conditioning systems in the buildings. The possibility of harvesting body heat as a renewable energy source to power a wearable personal heating system is investigated. The aim of this study is to integrate a wearable personal heating system with a thermoelectric generator (TEG) that harvests the body heat which is used to convert it into electricity. Moreover, the interaction between the TEG configuration and power output is studied. The power generation of TEG system is obtained by COMSOL Multiphysics software. The simulation results concluded that all the four proposed heat sink configurations can improve the power output of the wearable TEG at 1.4 m/s and 3m/s compared to that of the reference model. Furthermore, the perforated and trapezium shapes of heat sinks have a significantly better performance in comparison to conventional heat sinks.

1. Introduction

Due to global warming and lack of fossil fuel reservoirs, energy conservation measures are gaining more attention than any time before. Building sector is accounted for 36% of global final energy use and 40% of total direct and indirect CO_2 emission [1]. It is noteworthy that space heating attributes to the highest amount of energy consumption in the buildings [2]. For the time being, HVAC systems are the dominant space heating approach and are designed to provide a uniform thermal condition in the whole building regardless of individuals' thermal preferences [3]. This becomes more of a challenge when occupants share an office or a workspace, where the thermal preference varies from person to person.

An alternative is the application of Personalised Comfort Systems (PCSs), which distribute the conditioned air just around each individuals' body regarding their preferred temperature. There are four different types of personal heating systems, including heating chair, heating floor mat, heating desk mat, and heating garment. Among them, personal heating garment provides the highest thermal satisfaction with the lowest energy consumption [4]. Although, batteries have been the dominant energy source of heating garments, but they frequently add to the size and weight of the garments, and they need to be charged on a tight regular basis [5]. Therefore, it is desirable to replace the batteries

with a self-sustained and lightweight energy supply. One of the most promising alternative would be thermoelectric generators (TEGs), which have been being used as a power source of some wearable electronics such as motion detection and health monitoring [6]. However, due to low power output of TEGs, so far there have been no studies done on integrating a wearable thermoelectric generator with a personal heating garment to overcome the issues related to battery usage. As a result, this paper, which is a work in progress, aims to optimize the power generation of a wearable TEG to be able to power a personal heating garment.

1.1. Basic theories of wearable TEGs

As a warm blooded species, human body is a constant great source of thermal energy. Body temperature varies in a range of between 23 °C and 37 °C when room temperature fluctuates between 15 °C and 47 °C [7]. Wearable thermoelectric generators (TEGs) utilize the temperature difference between body skin and ambient to generate a low level of power current [8]. Figure 1 shows the standard configuration of a wearable TEG. As it can be seen, wearable TEGs consist of an array of p- and n-type semiconducting legs where the p type has surplus holes and the n-type has surplus electrons to carry the electrical current. The thermoelectric legs (semiconductors) are highly doped electrically in series and thermally in parallel through metal interconnects, which shape thermocouples. Finally, the thermocouples are sandwiched between two electrically insulating and thermally conductive substrates. The substrates that are placed on top and bottom of the thermoelectric legs are called cold and hot substrates respectively. Based on Seebeck effect, when a temperature gradient occurs across a thermoelectric leg, free charges (electrons and holes) in the leg start moving, which results in conversion of thermal energy into electrical energy. To accelerate heat dissipation and increase power generation, a heat sink (radiator) is also being attached above the cold plate [9]. As a rule of thumb, power generation of a thermoelectric module depends on the temperature difference between its hot and cold junctions. Higher temperature difference results in higher power generation. Since heat sink is the promising component of wearable TEGs due to its coolant mechanism, it is essential to evaluate its configuration effect on the power output of the wearable TEGs.

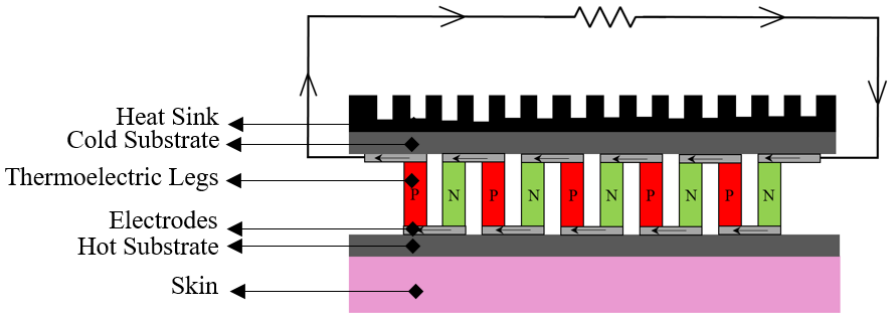

Figure 1. Schematic diagram showing components and arrangement of a typical wearable TE module.

2. Methodology

In the present work, the performance of four proposed configurations of heat sink is evaluated by COMSOL Multiphysics software. The modelled TEG representing the commercialized industrial Seebeck Effect Module GM 250-71-14-16 [10]. This traditional type of TEG has rigid metal interconnects (copper) and rigid top and bottom ceramic (Al_2O_3) substrates. It has 72 pairs of rectangular-shaped P-type and N-type thermoelectric legs with 1.4mm width, 1.4 mm length and 1.6 mm height. The electrodes and the substrates are respectively 0.1mm and 1mm thick. The thermoelectric legs are connected in series and thermally in parallel by the top and bottom copper strips. The dimension of the TEG is, 30 mm × 30 mm × 3.8 mm. Figure 2 shows a section through the

3D modelled heat sinks coupled with the off the shelf TEG. The heat sink with straight fins (model a) is a conventional configuration of a heat sink and is used as a reference model. In particular, the performance of the four designed models are compared with that of the reference model. Dimension of the fins is kept constant at 30 mm (length) × 1 mm (width) × 6 mm (height) for all five models. However, regarding the T shape fins, the height of the shorter fins is specified 4.5mm.

In fact, users of the personal heating garments, which are powered by a wearable TEG, conduct different activities throughout a day. Thus air flow speed regarding the users' activity is also considered as the studying variable. Accordingly, three different air speeds are considered for evaluation, including 0m/s (resembling a seated person), 1.4 m/s (resembling a walking person), 3 m/s (resembling a jogging person). In total, 15 samples are simulated and compared with each other in terms of maximum temperature of the heat sinks and power output of the wearable TEG. In addition, room and skin temperatures are set at 5°C (T_{cold}) and 24°C (T_{hot}) respectively.

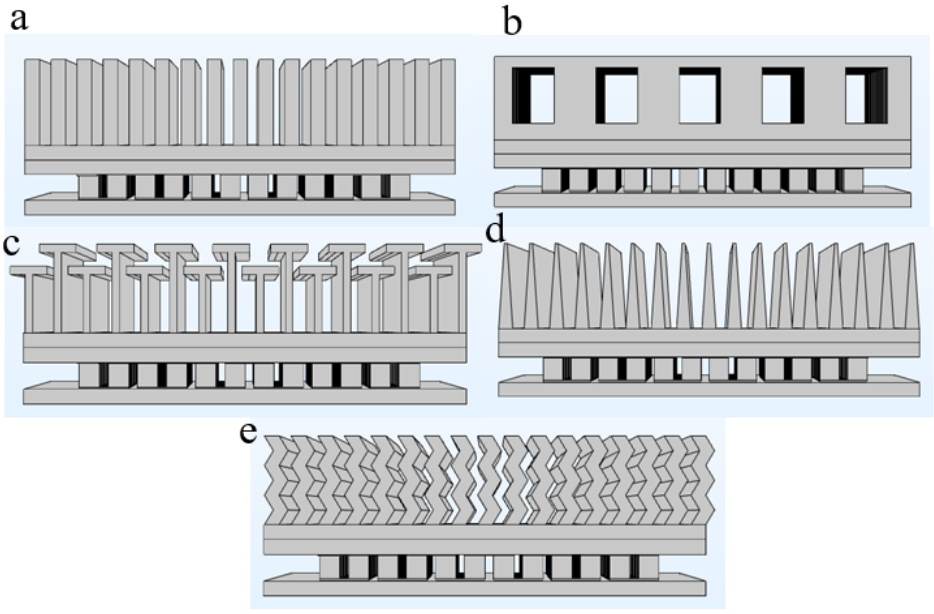

Figure 2. Schematic of the modelled heat sinks in COMSOL: (a) straight fins (b) perforated fins (c) T shape fins, (d) trapezium fins, and (e) wavy fins.

2.1. Governing equations

The thermoelectric effect is direct conversion of temperature difference to potential difference and visa versa. The governing equations for determining the thermoelectric effect in the Joule heating equation are Maxwell and heat diffusion equations, which should be solved simultaneously:
Maxwell equation:

$$\nabla . J = 0 \quad (1)$$

$$\mathrm{E} = -\nabla \mathrm{V} \quad (2)$$

where J is current density (in A/m^2), E is electeric field (in V/m) and V is electeric potential (in V). The time varing heat diffusion equation:

$$\rho C_p \frac{\partial T}{\partial t} + \nabla.q = Q \quad (3)$$

Here, ρ is density of material (in kg/m^3) , C_p is heat capacity (in J/(kg·K)) , T is temperature (in K), q is energy density heat flux (in W/m^2) and Q is the energy generation (in W). The related constitutive equations are

$$q = -k\nabla T + PJ \quad (4)$$

$$J = \sigma . (E - S.\nabla T) \quad (5)$$

$$Q = J.E \quad (6)$$

where P is peltier coefficient (in W/A) , S stands for Seebeck coefficient (in V/K), and k stands for thermal conductivity (in W/m·K). In this work, since heat diffusion is determined to be constant, Equation 3 can be simplified as:

$$\nabla.q = Q \quad (7)$$

2.2. Boundary conditions

The boundary condition is assumed as a constant value for the five simulated models as given in Figure 3. In addition, the following assumptions are made as follows:

- The thermal conductivity, Seebeck coefficient, and electrical conductivity are temperature independent.
- A constant temperature (T_{hot}) of 24°C is applied to the bottom surface of the hot substrates, which is equivalent with the body temperature in cold environment.
- The initial temperature of the TEGs is equal with outdoor temperature (T_{cold}), which is 5°C.
- In order to study the electric potential, one side of the n-type leg is grounded (V=0) assuming that the potential current flows from the p- type leg towards the n-type leg.
- No external electric potential passes through the module.

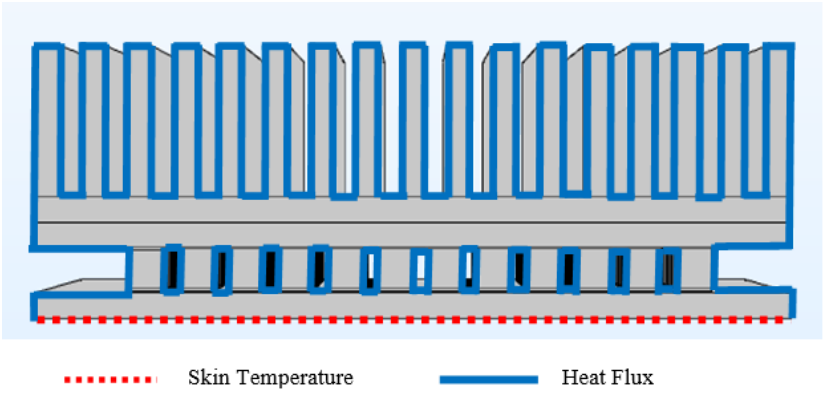

Figure 3. An illustration of the defined boundary conditions in the COMSOL Muliphysics.

2.3. Material properties

Most conventional TE devices use bismuth telluride (Bi_2Te_3) as a thermoelectric material, which are characterized by three parameters including Seebeck coefficient, electrical and thermal conductivities.

In addition, the heat sink, substrates and the interconnects are assumed to be made from aluminium (Al), aluminium oxide (Al_2O_3) and copper (Cu) respectively, which are the most common material in the structure of conventional TEGs. Table 1 summarizes some properties of the materials used in the simulation.

Table 1. The properties of materials used in the simulation.

Geometry	Material	α (V/K)	σ (S/m)	λ (W/mK)	ρ(kg/m^3)	c(J/kg*K)
P leg	p-Bi_2Te_3	$1.89e^{-4}$	$1.27e^{6}$	1.65	7700	154
N leg	n-Bi_2Te_3	$-2.1e^{-4}$	$1.08e^{6}$	1.67	7700	154
Electrode	Cu	-	$5.99e^{7}$	400	8960	385
Substrate	Al_2O_3	-	-	35	3965	730
Heat Sink	Al	-	$37e^{4}$	238	2700	900

3. Results

3.1. Heat flux

Figure 4 provides an arrow line plot indicating the heat flux pattern of the five models generated. As it can be seen, the highest amount of heat dissipation in all these five models is at the junctions, where the fins meet the horizontal plate. The reason is that the temperature difference between the junctions and ambient air is high, but it reduces as the heat moves across the fins. Apart from the junctions, straight and wavy shape fins achieve respectively the lowest and the highest heat dissipations. This is primarily because the surface area of the wavy fins is 491.8 mm^2, which is 60 mm^2 more than that of the straight counterpart. Thus, the folded surface of the wavy fins increases air exposure and accordingly enhances heat removal. Furthermore, the wavy shape fins result in heat release in various directions, whereas the straight fin dissipates heat only in parallel with the fin's edge. Likewise, adding a horizontal component on top of the straight fins not only enhances the air exposure, but also provides both vertical and diagonal heat dissipation. Thus, T shape is also an appropriate design of fins to enhance the performance of the heat sink. In contrast, creating holes in the fins or beveling them reduces the surface areas of perforated and trapezium shape heat sink. Therefore, it is likely that the heat dissipation from these two shapes be lower than that of the straight fins.

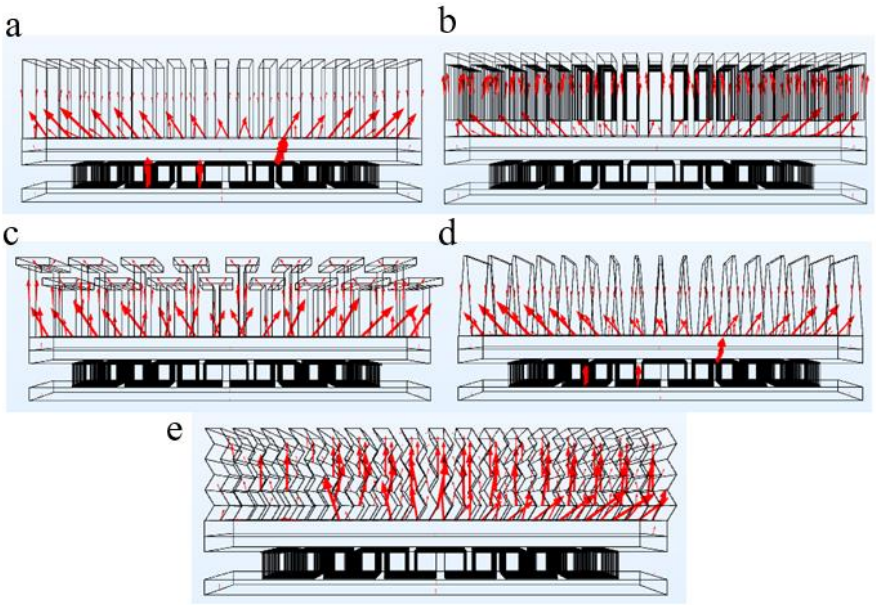

Figure 4. Arrow line plot of the modelled heatsinks in COMSOL: (a) straight fins (b) perforated fins (c) T shape fins, (d) trapezium fins, and (e) wavy fins.

3.2. Maximum temperature

Figure 5 illustrates the maximum temperature of the five modeled heat sinks under three different air speeds, including 0 m/s (a seated person), 1.4 m/s (a walking person) and 3 m/s (a jogging person). As it can be seen, the increasing air velocity remarkably decreases the temperatures of the fins in all specified models. This is because faster airflow accelerates heat dissipation from the fins to the ambient. Furthermore, the wavy and T shape fins achieve the lowest temperatures at all airflow speeds compared to the other models. As mentioned above, the primary reason of that is the greater surface area of these two models compared to their counterparts. Regarding the trapezium and perforated fins, their temperatures are higher than the straight fins at a steady state condition, which is attributed to their lower surface areas. Conversely, when air starts moving, the heat dissipations from the trapezium and perforated fins become significantly higher than that of the straight fins. A probable explanation is that air transfers easily through the fins due to the punched holes in the perforated fins and the funnel shape of the trapezium fins accelerates the heat movement along the fins. In total, under a steady air condition the temperature of the five models are almost the same. However, at air velocities of 1.4 m/s and 3 m/s, the four designed models achieve a remarkably lower temperature compared to the straight counterpart, which is desirable.

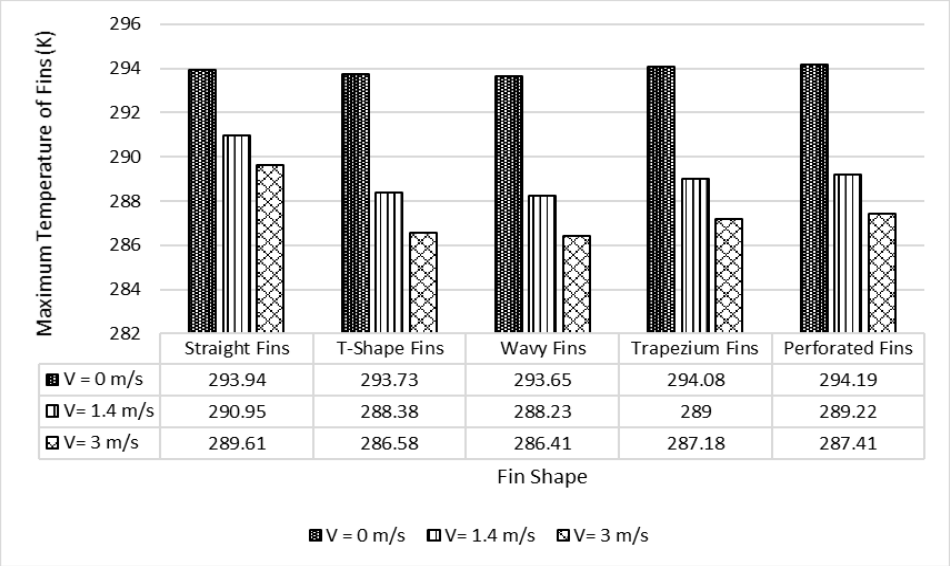

Figure 5. Comparison among the maximum temperature at three different air flow speeds.

3.3. Power generation

Figure 6 illustrates the power generated by the five studying models at different air speeds. As it can be seen there is a correlation between the air speed and the power output. Specifically, all five models generate the highest power at 3m/s air speed, while they achieve the lowest power outputs at a steady state condition. With regard to the fins' shape, the perforated and trapezium fins result in the lowest power generation with 0.2 m·W, when there is no airflow. However, in the same air condition, the maximum power is achieved by the T shape and wavy shape fins with 0.37mW. Likewise, at air speed of 1.4m/s and 3m/s, the T and wavy shapes are the dominant fins regarding the power output. However, unlike the air speed of 0m/s, the perforated and trapezium shape fins perform better than the straight fins at 1.4m/s and 3m/s. Indeed, these results comply significantly with the outcomes of the maximum temperature. Although the effect of the fins' shape on power output of a TEG is negligible at no air flow condition, but it is considerable when there is an air flow.

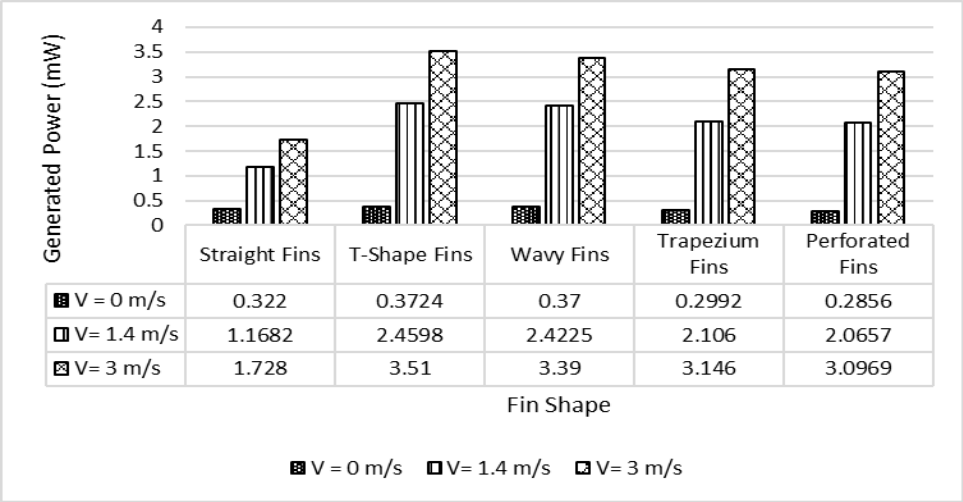

Figure 6. Comparison among power generation at three different air flow speeds.

4. Conclusion

Over the last few year, there have been a tremendous effort on improving personal heating systems. However, there is currently few of researches that have been done instead of the battery of these garments, such as a TEG. This study aims to enhance a wearable TEG power output and investigate four novel configurations to fulfil reliable energy source for personal heating garments. The performance assessments of these four heat sink configurations are obtained by COMSOL Multiphysics software. The results revealed that no airflow speed and difference configuration of the heat sinks result in the negligible effect on the TEG power generation. However, when the air flow speed reaches 1.4m/s and 3m/s, the heat sinks' configuration causes a remarkable difference in power generation. In particular, the T shape and wavy shape heat sinks achieve the highest power generation in all defined air flow speed senarios. However, the perforated shape and trapezium shape heat sinks have a significantly better performance than a conventional heat sink when air flows. It is believing that the work presented will contribute to enhancing power generation of the wearable TEGs for personal heating garments.

References

[1] https://www.iea.org/topics/energyefficiency/buildings/ Accessed 20 April 2019.
[2] https://wedocs.unep.org/bitstream/handle/20.500.11822/27140/Global_Status_2018.pdf?sequence=1&isAllowed=y Accessed 30 April 2019.
[3] Melikov AK 2016 Advanced air distribution: improving health and comfort while reducing energy use *Indoor Air* **26** (1) 24-112.
[4] Ziqi Li U, Ke Y, Wang F and Yang B 2018 A study of thermal comfort enhancement using three energy-efficient personalized heating strategies at two low indoor temperatures *Build Environ* **143** 1-14.
[5] Knecht K, Bryan-Kinns N and Shoop K 2016 Usability and design of personal wearable and portable devices for thermal comfort in shared work environments *Proceedings of the 30th International BCS Human Computer Interaction Conference* (Poole: Bournemouth University).
[6] Wang Y, Shi Y, Mei D and Chen Z 2018 Wearable thermoelectric generator to harvest body heat for powering a miniaturized accelerometer *Appl Energ* **215** 690-98.
[7] Thielen M, Sigrist L, Magnoc M, Hierold C and Benini L 2017 Human body heat for powering wearable devices: from thermal energy to application *Enrg Convers Manage* **131** 44-54.

[8] Leonov V and Vullers R 2009 Wearable electronics self-powered by using human body heat: The state of the art and the perspective *J Renew Sustain Ener* **1** (6).
[9] Gao H, Huang G, Li H, Qu Z and Zhang Y 2016 Development of stove-powered thermoelectric generators: A review *Appl Therm Eng* **96** 297-310.
[10] https://www.europeanthermodynamics.com/products/datasheets/GM250-71-14-16%20(2).pdf/ Accessed March 31 2019.